Research article

ES3
Earth Science, Systems and Society

https://doi.org/10.1144/esss2025-005 | Vol. 6 | 2026 | esss2025-005

Neoarchean gold grain size and artisanal mining in Migori, Kenya: review of current recovery methods

Clive J. Mitchell[1]*, Tom Bide[1], Cavince Odhiambo[2], Martin Nyakinye[3], Jeremy C. Rushton[1], Carolin Kresse[4] and Monty Pearson[1]

[1] British Geological Survey, Keyworth, Nottingham NG12 5GG, UK
[2] Flux Carbon, Nairobi, Kenya
[3] Ministry of Petroleum and Mining, Nairobi, Kenya
[4] Bundesanstalt für Geowissenschaften und Rohstoffe, Berlin, Germany
CJM, 0000-0002-5911-5668; TB, 0000-0002-5752-0723; JCR, 0000-0001-5931-7537; MP, 0000-0002-0295-9552
* Correspondence: cjmi@bgs.ac.uk

Abstract: Artisanal and small-scale gold mining (ASGM) in Archean greenstone provides a significant source of income for rural communities. Understanding of the particle size distribution of gold is an important parameter for its recovery as it determines the most appropriate and effective mineral processing methods. However, published information is scarce. This study set out to determine the particle size distribution of gold in the ASGM areas in Migori, SW Kenya. The Neoarchean Migori Greenstone Belt in SW Kenya hosts the 'Migori Goldbelt'. Gold mainly occurs in coarsely crystalline quartz 'reef' veins associated with sulfide mineralization as well as in banded iron formations and more disseminated in tuffaceous rocks. Based on scanning electron microscope grain count data, the mean particle size of the gold grains was found to be 3.5 µm, too fine-grained for effective recovery by sluice boxes. Taking the weight of the gold particles into consideration, 80% of the weight of the gold is coarser than 15 µm and could be recovered using a shaking table. Adopting improved ASGM practices would increase the recovery of fine-grained gold and help to reduce the amount of hazardous substances used in the recovery process. Improved gold recovery would help to boost local economies, secure livelihoods and enhance the quality of life for ASGM communities.

Keywords: gold; artisanal mining; liberation; recovery; greenstone belt.

Received 11 April 2025; **revised** 11 March 2026; **accepted** 11 March 2026

Artisanal and small-scale gold mining (ASGM) is defined by the Minamata Convention on Mercury as gold mining conducted by individuals or small enterprises with limited capital investment and production (UNEP 2019). It is estimated to be responsible for 20% of the world's annual gold supply (World Bank 2019). It is widespread in many Archean greenstone belt terranes across the world, particularly in Africa, Asia and South America (Intergovernmental Forum on Mining Minerals Metals and Sustainable Development 2017). Greenstone belts are often referred to as 'gold belts' as they host many significant gold deposits with notable concentrations of large-scale mining operations in Africa, Canada and Western Australia. Despite the large amount of published research on greenstone belts and associated gold mineralization, there is relatively little published information on the particle size distribution of the gold. The particle size of gold is arguably one of the most important parameters in the selection of the appropriate techniques for the recovery of gold.

Artisanal and small-scale gold mining areas typically use simple gravity processing methods such as panning and sluicing to recover gold by exploiting its high density. These simple gravity methods are ideal for the recovery of alluvial gold, as it is relatively coarse-grained (typically in the size range 300–1500 µm) and can be captured effectively by meshes and mats. Gold that occurs in greenstone belts, often referred to as 'hard rock' gold, is very fine-grained (typically less than 100 µm, with a significant proportion finer than 10 µm). The recovery rate of a sluice box is as low as 20% for gold finer than 100 µm (Mitchell *et al.* 1997). A high proportion of the fine-grained gold in greenstone belt ASGM areas is lost if gold recovery methods such as panning and sluicing are used. The loss of fine-grained gold represents a poor financial return for the hard work and risks taken by the rural farmers or migrant labourers that typically make up ASGM communities and may result in higher throughput of material and the associated negative environmental impacts that are associated with ASGM.

This study aimed to determine the particle size distribution of gold in the ASGM areas in Migori, SW Kenya. The relationship between the particle size of gold and the processing methods used is an aspect largely overlooked in work aiming to improve ASGM practices. A better understanding of the particle size properties of gold would enable the selection of the most appropriate processing practices and provide evidence for a change in mining practice to help improve gold recovery rates, increase the income for ASGM communities and reduce the environmental impacts of mining.

Greenstone belts and gold

Greenstone belts are deformed and metamorphosed volcano-sedimentary successions that occur as elongated slivers enveloped by granitic and gneissic rocks and are confined to the Archean, which ranges from the Eoarchaean (4–3.6 Ga) to the Neoarchean (2.8–2.5 Ga). It is a term synonymous with 'schist belt' and 'gold belt', in which significant gold deposits have been found in many parts of the world (Anhaeusser 2014). The gold deposits are predominantly epigenetic (i.e. formed later than the host rock), structurally controlled by fold and fracture systems and metamorphosed in the range of greenschist facies to amphibolite. Gold mineralization typically occurs in quartz and quartz–carbonate veins and fractures. Sulfide minerals are common, including pyrite,

Table 1. Particle size of gold in greenstone belt-hosted gold deposits

Gold deposit	Gold particle size	Reference
Boddington gold deposit, Saddleback Greenstone Belt, Western Australia	<20 µm	Kalleske (2010)
Buck Reed gold mine, Nyanzian Greenstone Belt, Mwanza, Tanzania	<15 µm	Kinabo (1991)
Fold Gold deposit, Midlands Greenstone Belt, Zimbabwe	<20 µm	Buchholz *et al.* (1998)
Klein Letaba gold mine, Sutherland Greenstone Belt, South Africa	1–15 µm	Gan and Van Reenen (1997)
Musoma–Mara Greenstone Belt, NW Tanzania	10–37 µm	Yuan *et al.* (2019)
Oleninskoe gold deposit, Kolmozero-Voronya Greenstone Belt, Kola Peninsula, Russia	200–300 µm	Lukonin (2008)
Orivesi gold deposit, Palaeoprotozoic Tampere Schist Belt, southern Finland	<20 µm	Kinnunen (2008)
Wasamac gold deposit, Abitibi Greenstone Belt, Canada	5.7 µm	Mériaud and Jébrak (2017)
Xiajinbao gold deposit, Eastern Hebei, China	5–53 µm	Wang *et al.* (2018)

arsenopyrite and pyrrhotite (Anhaeusser 2014). The gold is thought to come from a combination of partial melting of deep crustal rocks, mobilization in sulfide phases and interactions with related later stage granitic bodies (Foster and Piper 1993).

The gold particles found in greenstone belt-hosted gold deposits are typically finer than 15–20 µm (Table 1). In the Musoma–Mara Greenstone Belt in NW Tanzania, gold is hosted in pyrite within sericitized wall rocks, or in quartz veins occurring as inclusions and intergranular grains between 10 and 37 µm in size (Yuan *et al.* 2019). The Buck Reed gold deposit, located in the Nyanzian Greenstone Belt near Mwanza in NW Tanzania, has gold particles on average smaller than 15 µm locked in pyrite (Kinabo 1991).

Gold mining in the Migori Greenstone Belt

Gold was discovered in the Tanzanian Craton (an area of Archean basement rocks extending from Tanzania to eastern Kenya and southern Uganda) at the beginning of the twentieth century. Since then the region has been a significant gold producer, mostly in Tanzania, with only minor production from Kenya and Uganda.

The Migori Greenstone Belt, the most northerly of those occurring in the Tanzanian Craton, is 20 km wide and extends for 80 km along a NW to SE strike from the Tanzanian border to the Winam Gulf. The belt consists of a Neoarchean succession of dominantly metavolcanic rocks (referred to as Nyanzian) and younger dominantly metasedimentary rocks (referred to as Kavirondian), including pelites, psammites, tuffs, basalts, dacites, dolerites, andesites and rhyolites (Shackleton 1945). The Migori Greenstone Belt is dated at 2.85–2.3 Ga (Ichang'i 1993; Borg and Shackleton 1997) and is bounded, parallel to strike, by younger Neoarchean granites to the north and the Migori granite to the south (Fig. 1). In the Nyanzian rocks, greenschist metamorphism is ubiquitous with amphibolite facies at the contacts with the major granitic intrusions (Ichang'i and MacLean 1991).

Gold mineralization has a complex formation history; it occurs in steeply dipping, strike parallel quartz veins (known as 'reefs')

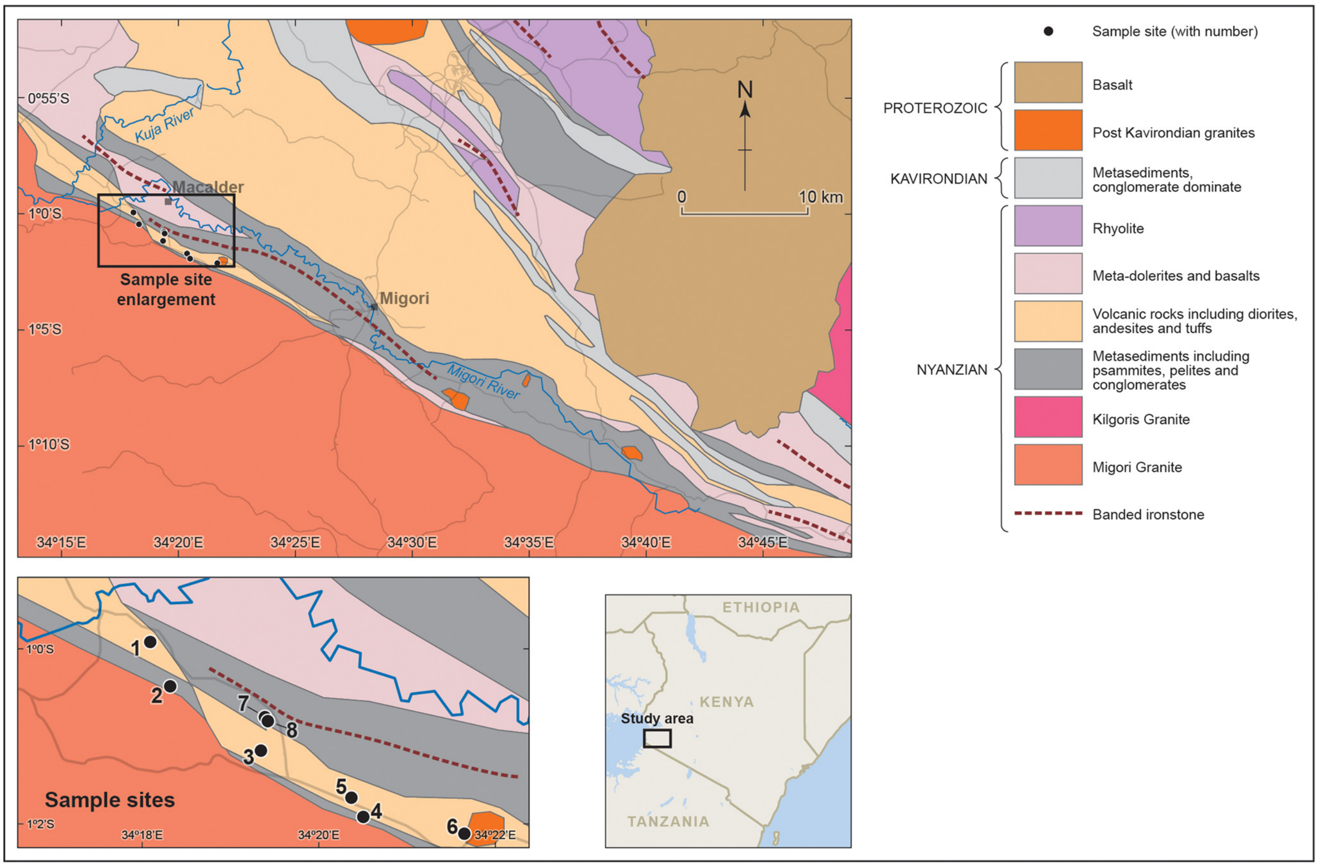

Fig. 1. Geology of the Migori Goldbelt and sample locations from mining sites visited for this study. Adapted from Shackleton (1945), Ichang'i and MacLean (1991) and Huddelston (1951).

Fig. 2. Sluice box in the artisanal gold mining area of Kehancha, Migori County, Kenya.

within the pelites, andesites and tuffs, in quartz veins oblique to the main greenstone belt strike, in banded iron formations and disseminated in tuffaceous rocks (Shackleton 1945; Sanders 1964; Ogola 1987, 1993; Ichang'i 1993). The gold mineralization is mainly associated with sulfide minerals (pyrite, pyrrhotite, chalcopyrite, arsenopyrite, sphalerite and galena) and occasionally magnetite (DuBois and Walsh 1970). Gold occurs along micro-fractures in pyrite and as inclusions in arsenopyrite (Ogola 1993). The close proximity of the gold-bearing veins to the Migori Granite indicates that the mineralization was probably due to fluids generated by the granitic intrusion circulating through the metal-rich volcano-sedimentary succession of the greenstone belt (Ogola 1987; Ichang'i 1993; Ogola *et al.* 2002).

Major commercial gold working took place in Migori between 1922 and 1996, with a total gold production of 4284 kg (Ogola 1993; Ogola *et al.* 2002). The majority of current day gold mining in Migori is artisanal or small scale with a large number of sites clustered around the quartz veins that occur near the Migori Granite contact. Drifts, pits or vertical shafts of varying depths are typically used to access the gold-bearing reefs. The ore is worked in cramped and poorly ventilated tunnels, some of which require pumping to keep them dry. The tunnels are supported by wooden beams. There are relatively frequent mine collapses, often leading to fatalities. Explosives are used to extract the ore, which is hauled out by hand in 25 kg sacks. The gold ore is crushed manually and then milled to a very fine particle size using small, locally produced, Tanzanian-designed ball mills driven by diesel engines.

The milled ore is processed using sluice boxes to produce gold-bearing concentrates (Fig. 2). A sluice box is a simple gravity-based mineral processing method that uses the high specific gravity of gold (19.3 g cm^{-3}) to separate it from the less dense minerals (Styles *et al.* 2002). Sluice boxes are typically built of wood with a rudimentary wooden feed box lined with hessian sacking to capture the gold. The sluice box concentrates are panned with mercury to concentrate the gold. Gold forms an amalgam with mercury. Excess mercury is removed by squeezing the amalgam in a cloth. The final gold–mercury amalgam has the consistency of putty and is 'cooked' over an open fire. The mercury is driven off from the amalgam to form a small porous ball of 'sponge' gold. This process is responsible for releasing a significant amount of mercury into the environment.

The tailings from ASGM are re-processed multiple times using sluice boxes to recover more gold. Ultimately the spent tailings are sold to the operators of leaching plants who use cyanide to recover residual gold. The tailings are shovelled into large cylindrical concrete lined tanks and a solution of sodium cyanide is added. Gold forms a complex with the cyanide (aurocyanide), which is water soluble. The gold-enriched leachate from these tanks is then passed over a separate series of smaller concrete tanks which contain activated charcoal. The gold cyanide complex is adsorbed onto the surface of the activated charcoal. This is removed from the charcoal by washing (typically with a caustic soda solution). The gold is produced from the gold-rich solution by electrowinning, further washing and smelting. This process is known as carbon-in-pulp.

The only major gold mine in the Migori Goldbelt is Kilimapesa, operated by Caracal Gold PLC, at the south-eastern end of the Migori Greenstone Belt, which is working gold hosted in a banded iron formation.

Materials and methods

In November 2019, the British Geological Survey (BGS) and the Department of Geology, University of Nairobi, with the assistance of Migori County Artisanal Miners Co-operative (MICA), visited mining sites in the Migori ASGM district. Representative samples of ore hand specimens, crushed and milled ore, and sluice box concentrates and tailings were collected from six ASGM sites. In addition, two sets of samples of shaking table concentrate, middling products and tailings were collected from the MICA demonstration gold processing plant (Table 2). Sample size selection was dictated by the limited access allowed by the artisanal miners with representative samples collected where possible. Simple coning and quartering was used to ensure that representative material was collected.

Analysis methodologies

Petrographical and micro-chemical analyses were carried out on polished thin sections of the ore. Optical microscopy was carried out using a Zeiss Axio Imager microscope in transmitted and reflected light mode to examine the gangue and ore minerals. Scanning

Table 2. ASGM sample sites in Migori, Kenya

Locality	Lithology	Geology
ASGM sites		
1. Mikeyi	Coarsely crystalline quartzite	Masara Andesitic Series – andesitic crystal tuffs
2. Kakula, Mikei	Coarsely crystalline quartzite	Nyanzian Shale in Metamorphic Aureole of Granite
3. Kolongo, Masara	Coarsely crystalline quartzite	Masara Andesitic Series – andesitic crystal tuffs
4. Masara	Fine grained metavolcanic rock	Masara Andesitic Series – andesitic crystal tuffs
5. Masara	Fine grained metavolcanic rock	Tuffaceous and slaty rocks
6. Mukuru	Fine grained metavolcanic rock	Masara Andesitic Series – andesitic crystal tuffs
MICA processing plant		
7. Kabobo	Coarsely crystalline quartzite	Tuffaceous and slaty rocks
8. Kabobo	Coarsely crystalline quartzite	Tuffaceous and slaty rocks

ASGM, Artisanal and small-scale gold mining; MICA, Migori County Artisanal Miners Co-operative.

electron microscopy (SEM) analysis was carried out using a Zeiss Sigma 300 field emission gun SEM fitted with energy dispersive X-ray detectors with Zeiss Mineralogic phase-mapping software. Samples were given an electrically conductive carbon coating and examined under high vacuum conditions. Backscatter electron photomicrographs were obtained as 8-bit greyscale TIF format images.

Phase mapping was carried out by SEM with a beam step size of 1.5 µm and a dwell time of 10 ms to map high brightness phases and the surrounding material. Phase identification, based on normalized quantitative energy dispersive X-ray data, was used to count the number of gold grains present (i.e. grain count). A mosaic of images was used to create a phase map of each thin section. Phase shape, size, position, association and liberation data were all derived using protocols built into the Mineralogic software. The effective diameter of the gold grains provides an appropriate measure of particle size. The weight distribution of the gold present was estimated using the effective diameter to calculate the volume (assuming the particles are spheres), which is equivalent to the weight distribution.

Mineralogical analysis was carried out on the milled ore by X-ray diffraction analysis using a PANalytical X'Pert Pro series diffractometer. Diffraction data were analysed using PANalytical X'Pert HighScore Plus version 4.9 software coupled to the latest version (at the time of analysis) of the International Centre for Diffraction Data database.

The gold content of the crushed and milled ore, sluice box concentrates and tailings, and shaking table concentrates, middlings and tailings samples was determined by fire assay and inductively coupled plasma–emission spectroscopy at the laboratories of Bureau Veritas in Canada. The lower limit of detection for gold was 2 ppb and the upper limit was 10 ppm. Where the gold content exceeded the upper limit of detection for inductively coupled plasma–emission spectroscopy, gravimetric analysis was used to determine the gold content. For gravimetric analysis the lower limit of gold detection was 0.9 ppm with no upper limit.

The particle-size distribution of the crushed and milled ore, and the tailings was carried out by wet sieving. The following sieve series was used: 20 mm, 16 mm, 8 mm, 4 mm, 2 mm, 1 mm, 500 µm, 250 µm, 125 µm and 63 µm. The particle-size distribution of the sub-sieve material (finer than 63 µm) was determined by X-ray sedigraph analysis.

Results

Petrography and mineralogical composition of gold ore

The ore samples taken by this study predominantly comprise multiphase hydrothermal vein deposits dominated by quartz and feldspar with extensive alteration in the form of chlorite and carbonate.

The only exceptions are from sites five and six, which may represent highly altered pelitic and andesitic country rock, respectively, or fragments of country rock within fractured vein material. All ore samples were from underground workings in areas of steeply dipping pelitic and meta-felsic rock with varying degrees of alteration (ranging from comparatively fresh outcrops to disaggregated gossans). Host rock lithologies of underground workings were identified by comparison with the observed outcrop at the surface and inference from geological maps (Shackleton 1945).

Gangue minerals consist mostly of quartz, albite and mica (mostly muscovite with rare biotite), with smaller amounts of carbonate (mostly calcite with rare dolomite and ankerite), chlorite (clinochlore), K-feldspar (microcline and orthoclase), hornblende and iron oxides. The samples commonly have coarse-grained quartz and occasionally hornblende in a fine matrix of recrystallized quartz and carbonate (Fig. 3a, c and e). Chlorite is ubiquitous, occasionally dominant with sericite (Fig. 3b) and rare amounts of kaolinite and smectite (Table 3). Accessory minerals include apatite (including thorium-rich apatite), monazite, scheelite, titanite, tourmaline and zircon.

The main ore mineral is arsenopyrite with smaller amounts of galena, gold, pyrite, pyrrhotite, silver and sphalerite. Gold occurs in association with arsenopyrite, in equilibrium with hydrothermal quartz (Fig. 3f), disseminated throughout the quartz/carbonate matrix (Fig. 3d) and associated with chlorite. Sulfides occur as either a fine-grained groundmass (Fig. 3c) or coarse-grained and euhedral crystals (Fig. 3b).

Particle size and liberation characteristics of gold in ore

The primary gold-bearing phase identified was electrum, a gold-rich natural alloy of gold and silver, which is defined in this study as gold containing greater than 11 wt% silver. The composition of the electrum ranges from 71 to 88% gold and from 12 to 29% silver. In addition, there was a small amount of gold with less than 11% silver. Pure gold was relatively rare. The electrum and other gold-bearing grains are collectively referred to as gold here. The SEM grain count identified 5675 gold grains.

Gold typically occurs in fractures, some associated with growth rings, in arsenopyrite (Fig. 3a) and the alteration products of arsenopyrite (tentatively identified as arsenosiderite or hydrated oxide/ hydroxide) (Fig. 4). A small amount of gold is associated with chlorite, galena and quartz.

The particle size and weight distribution of the gold grains are based on all of the data from the whole rock ore samples analysed by SEM (Table 4 and Fig. 5). The grain count is the number of grains identified as electrum or gold in polished thin sections. The weight percentage is equivalent to the volume calculated from the equivalent diameter assuming the grains have a spherical shape. This shows that 87% of the total gold grain count is finer than 6 µm. Gold coarser than 15 µm represents 80% of the weight of the gold but less than 2% of the total grain count.

The 'liberation size' of the gold is a key parameter in mineral processing. This represents the particle size at which an acceptable proportion of the gold is detached from the surrounding impurities during crushing of the ore. The 'fractional liberation' of gold was calculated from the mean particle size of the gold. This gives an estimate of the percentage of gold liberated at different grind sizes (King 1979; Finch and Petruk 1984). The mean particle size of the gold grains by weight is 45 µm. If the ore is ground to less than 100 µm, the fractional liberation is 48%. Higher liberation occurs at finer grind sizes, with over 90% fractional liberation at 10 µm (Fig. 6).

Data on the full particle size distribution for gold from greenstone belt-hosted gold deposits are comparatively scarce in published literature. In Figure 6 the gold particle size distribution is shown for the Orivesi gold deposit in southern Finland and the Xiajinbao gold deposit in Eastern Hebei, China (Kinnunen 2008; Wang *et al.* 2018). There is, however, no consideration given in these studies to the weight distribution of gold rather than grain count size distribution. The availability of full particle size weight distribution data is important as it enables the determination of the liberation size and the methods of processing that are required for the effective concentration and recovery of the gold.

The minimum, optimum and practical grind sizes were also calculated. The minimum grind is the particle size at which 80% (D_{80}) of the mass of the gold particles is finer (Fig. 3). The optimum grind is the size at which the incremental increase in mineral liberation becomes minimal with decreasing particle size. The practical grind is a compromise between the minimum and optimum grind sizes (Petruk 1986). The minimum grind size is 88 µm, which results in a fractional liberation of 52%; the optimum grind size is

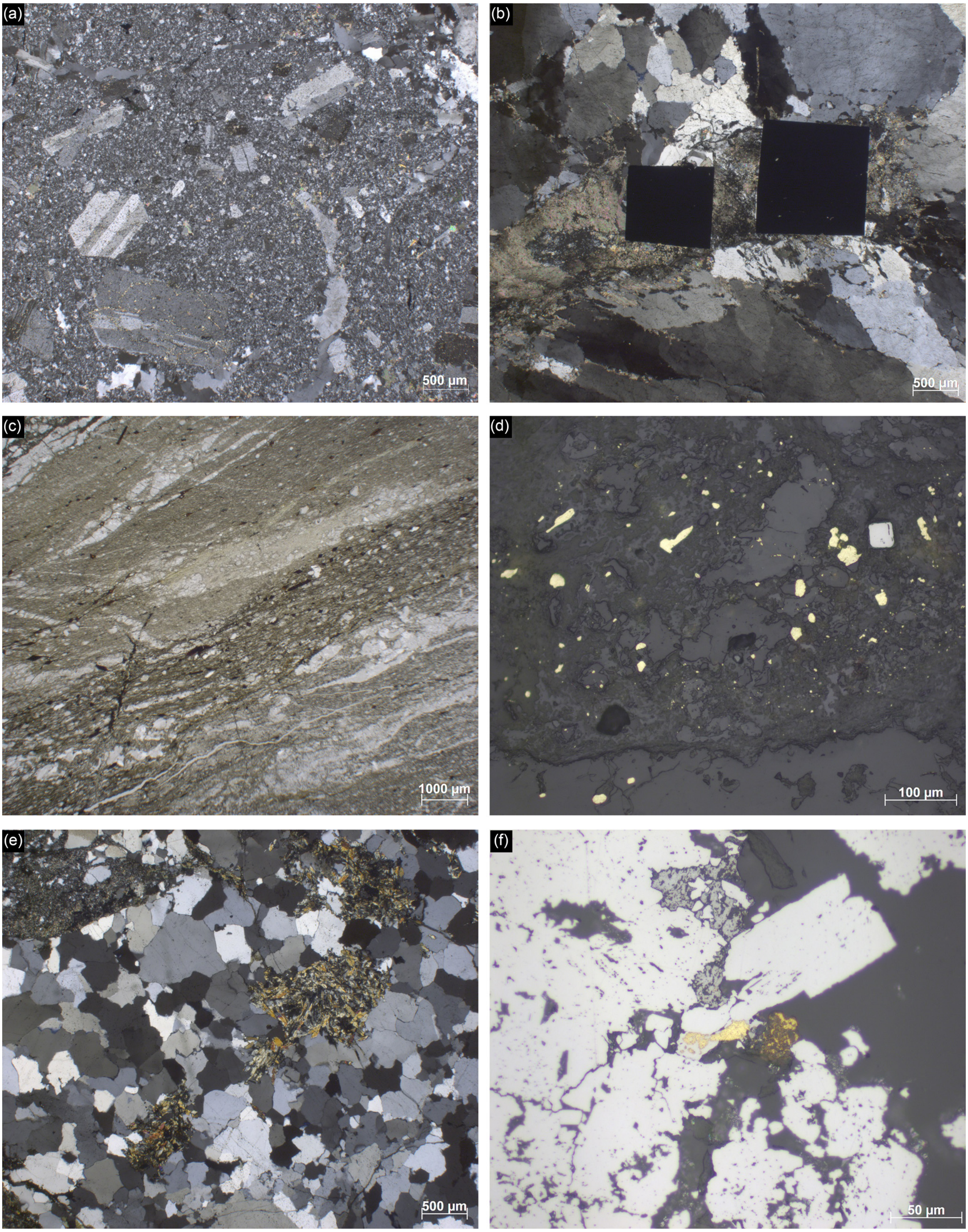

Fig. 3. (**a**) Medium-to large grained quartz and plagioclase phenocrysts and fine crystalline quartz-carbonate matrix (transmitted light crossed polarisers) (site 1). (**b**) Euhedral sulphide grains associated with chlorite alteration (transmitted light crossed polarisers) (site 3). (**c**) Fine-grained quartz–carbonate–chlorite matrix, disseminated sulphide minerals (opaque) (transmitted light) (site 4). (**d**) Disseminated free gold (~50 µm in size) associated with chlorite alteration with a single sulphide grain (white) (reflected light) (site 6). (**e**) Fine- to medium-grained quartz, very fine-grained carbonate and chlorite (transmitted light) (site 7). (**f**) Sulphide in equilibrium with gold (reflected light) (site 7).

Table 3. Mineralogical composition of milled ore, Migori County, Kenya

Mineral	Site 1 wt%	Site 2 wt%	Site 3 wt%	Site 4 wt%	Site 5 wt%	Site 6 wt%	Site 7 wt%	Site 8 wt%
Quartz	35.6	81.4	58.2	69.8	58.5	50.4	76.8	82.3
Albite	56.9	3.9	26.5	15.2	11.9	27.5	3.6	3.2
Muscovite	4.1	14.3	8.3	11.5	17.1	8.6	13.5	13.0
Microcline	0.0	0.0	0.0	0.2	6.1	10.4	0.1	0.2
Clinochlore	0.0	0.0	3.9	1.0	0.4	2.1	0.8	0.4
Calcite	2.0	0.0	2.9	1.2	0.0	0.0	0.0	0.0
Dolomite	0.0	0.0	0.0	0.0	0.1	0.0	5.0	0.4
Amphibole	0.0	0.0	0.0	0.0	4.3	0.0	0.0	0.0
Sulfides	0.3	0.4	0.2	0.1	0.9	0.3	0.2	0.3
Smectite	0.0	0.0	0.0	1.0	0.7	0.0	0.0	0.0
Ankerite	1.1	0.0	0.0	0.0	0.0	0.0	0.0	0.0
Orthoclase	0.0	0.0	0.0	0.0	0.0	0.7	0.0	0.0

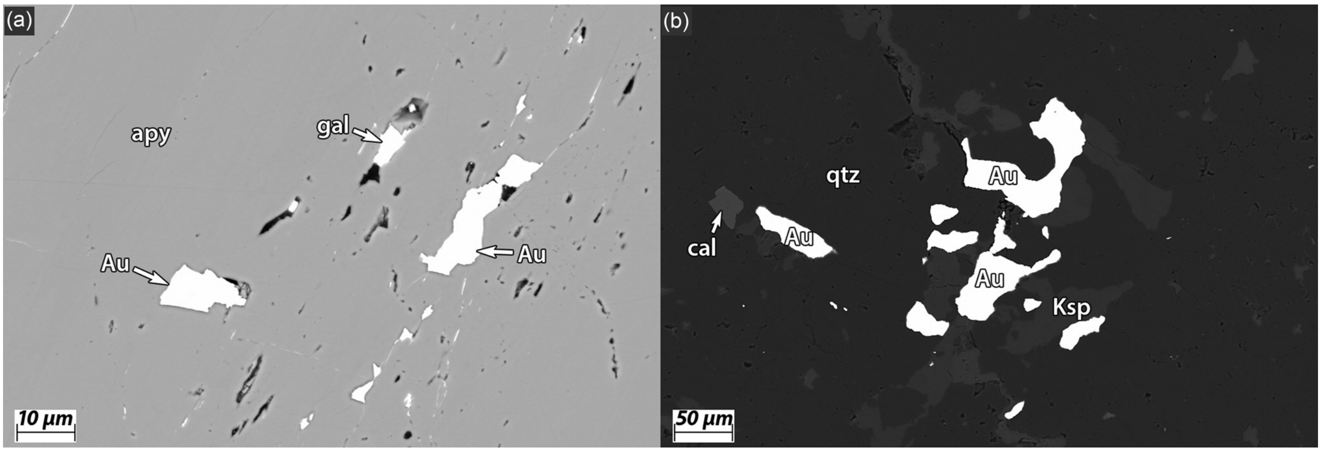

Fig. 4. Backscatter electron images: (**a**) showing gold (Au) and galena (gal) hosted in arsenopyrite (apy) and (**b**) showing gold (Au) hosted in intergrown quartz (qtz) and K-feldspar (Ksp).

6 µm, giving 95% liberation;and the practical grind size is 37 µm, giving 73% liberation (Fig. 7).

Particle size and gold distribution in ASGM processing products

The crushed ore consists of 88% gravel-sized particles and the milled ore is 97% finer than 500 µm (Fig. 8). The milled ore has a mean D_{80} of 172 µm, which represents a fractional liberation of 35 wt% of the gold. The particle size distribution of the milled ore shows a significant proportion of particles that are too fine grained (65% finer than 100 µm) for efficient gravity recovery of gold using a sluice box.

Gold assays of the ASGM products are variable but do show a significant difference in the amount of gold recovered using different mineral processing methods. Sluice box processing has a mean concentration ratio of 2.5 with a mean gold content in the milled feed of 17.6 g t^{-1} and in the concentrates of 49.1 g t^{-1}. In comparison, shaking table processing had a mean concentration ratio of 66.7 with a mean gold content in the milled feed of 9.1 g t^{-1} and in the concentrates of 316.1 g t^{-1} (Table 5).

Table 4. Gold grain size distribution in ore, Migori County, Kenya

Particle size	Distribution of gold grains in ore		
	Grain count		Weight distribution (%)
	Number	Distribution (%)	
125–63 µm (very fine sand)	2	0.04	40.26
63–20 µm (coarse silt)	39	0.69	33.07
20–6 µm (medium silt)	654	11.52	22.00
6–2 µm (fine silt)	2424	42.71	4.27
<2 µm (clay)	2556	45.04	0.40
Total	5675	100.00	100.00

Discussion

This study set out to determine the particle size distribution of the gold in the ore samples worked by ASGM in Migori. It is important to recognize that grain size analysis based on grain counts does represent the distribution of gold grains but does not represent the weight distribution of gold in the ore. Assuming the gold grains have a spherical shape, a gold grain that is 100 µm in diameter is 125 times heavier than a gold grain that is 20 µm in diameter. If a sample contains an equal proportion of 100 and 20 µm-sized gold grains, the larger gold grains would represent over 99% of the weight of gold present.

The grain count data would appear to indicate that the gold in Migori is far too fine for effective recovery using a gravity-based mineral processing method. Based on the grain count for the ore samples from Migori, the gold has a mean particle size of 3.5 µm and 96% of the gold grains are finer than 10 µm. Sluice boxes, such as those used in Migori, have an effective size range of 100–2500 µm for the recovery of gold grains. Recovery efficiency drops to less than 20% for gold grains finer than 100 µm.

However, if the weight of the gold particles is taken into consideration, the mid-point in the particle size distribution of the

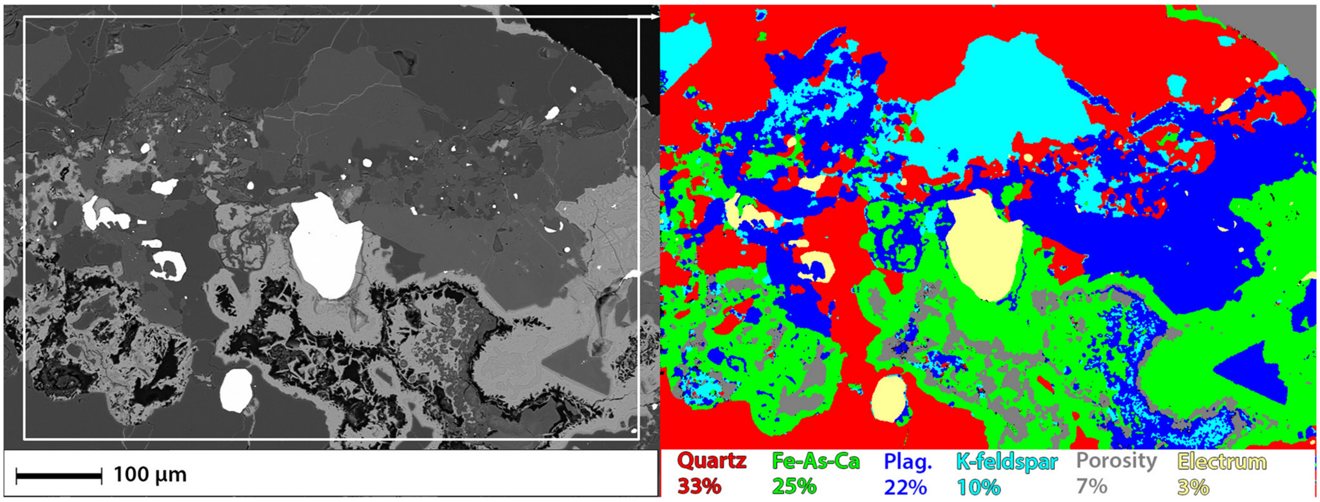

Fig. 5. Backscatter electron image (**a**) and associated false coloured mineral phase map (**b**) showing electrum hosted in an alteration product (possibly arsenopyrite with quartz and feldspar).

gold grains is 45 µm and 80% of the weight of the gold is in the size range 15–100 µm. This has a significant implication for the recovery of gold using a gravity-based method. Whereas this is still too fine for effective gold recovery using sluice boxes, it is possible using shaking tables, which have an effective size range of 15–3000 µm for the recovery of gold (Mitchell *et al.* 1997). The poor recovery using sluice boxes is borne out by the poor concentration ratio (2.5) of gold recovered by sluice boxes in Migori. Recovery of gold using the shaking table at the MICA demonstration plant in Migori was more effective with a significantly higher concentration ratio (66.7).

Implementation of the following good practice guidance (based on Mitchell *et al.* 2023). would help to improve the gold recovery of the existing ASGM operations in Migori:

- Ball milling of gold ore tends to over-grind a proportion of the feed material. Approximately one-third of the gold ore that has been ball milled by the ASGM operations in Migori

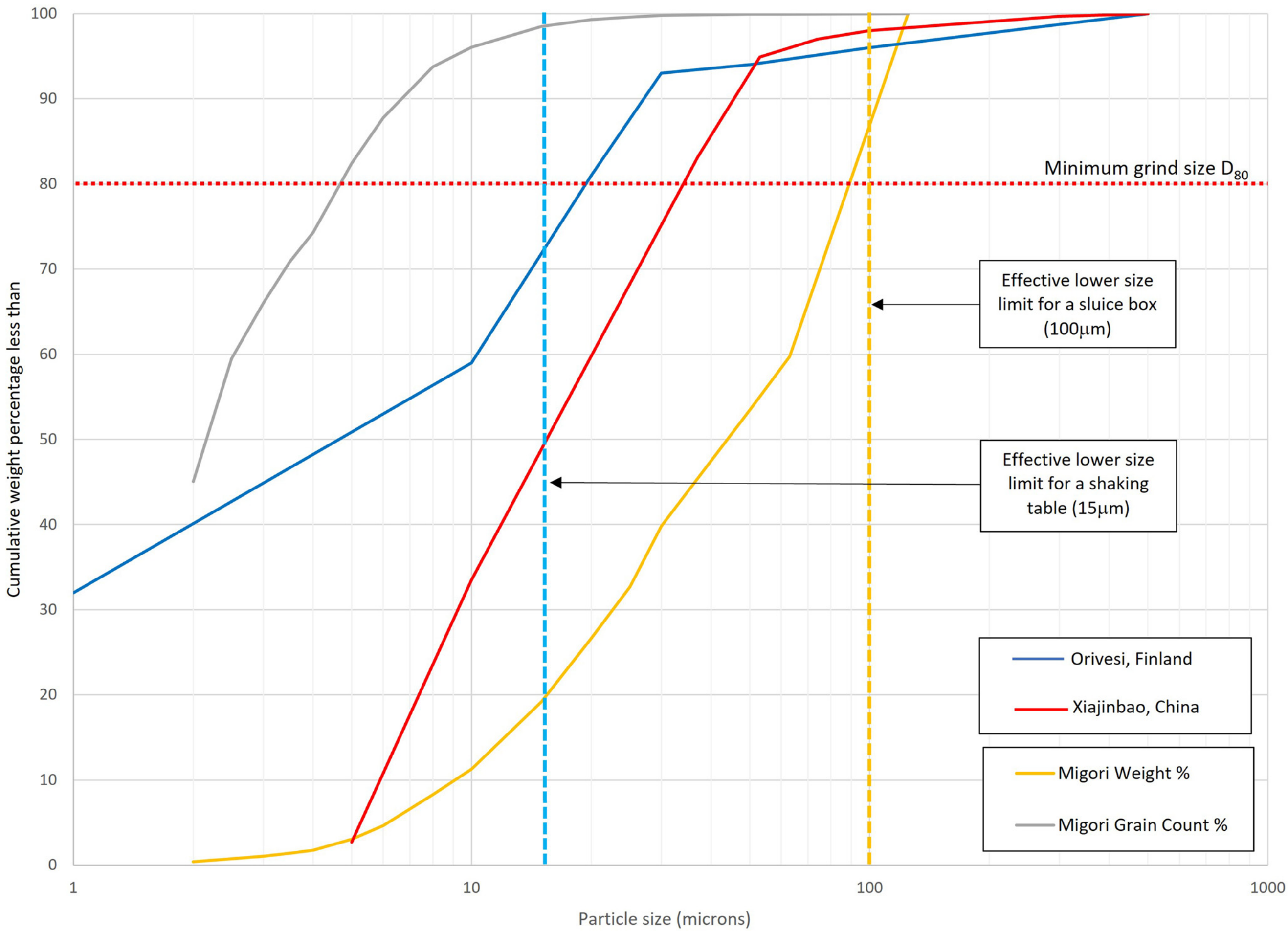

Fig. 6. Distribution of gold in ore, Migori County, Kenya, compared to published grain count data (Kinnunen 2008; Wang *et al.* 2018).

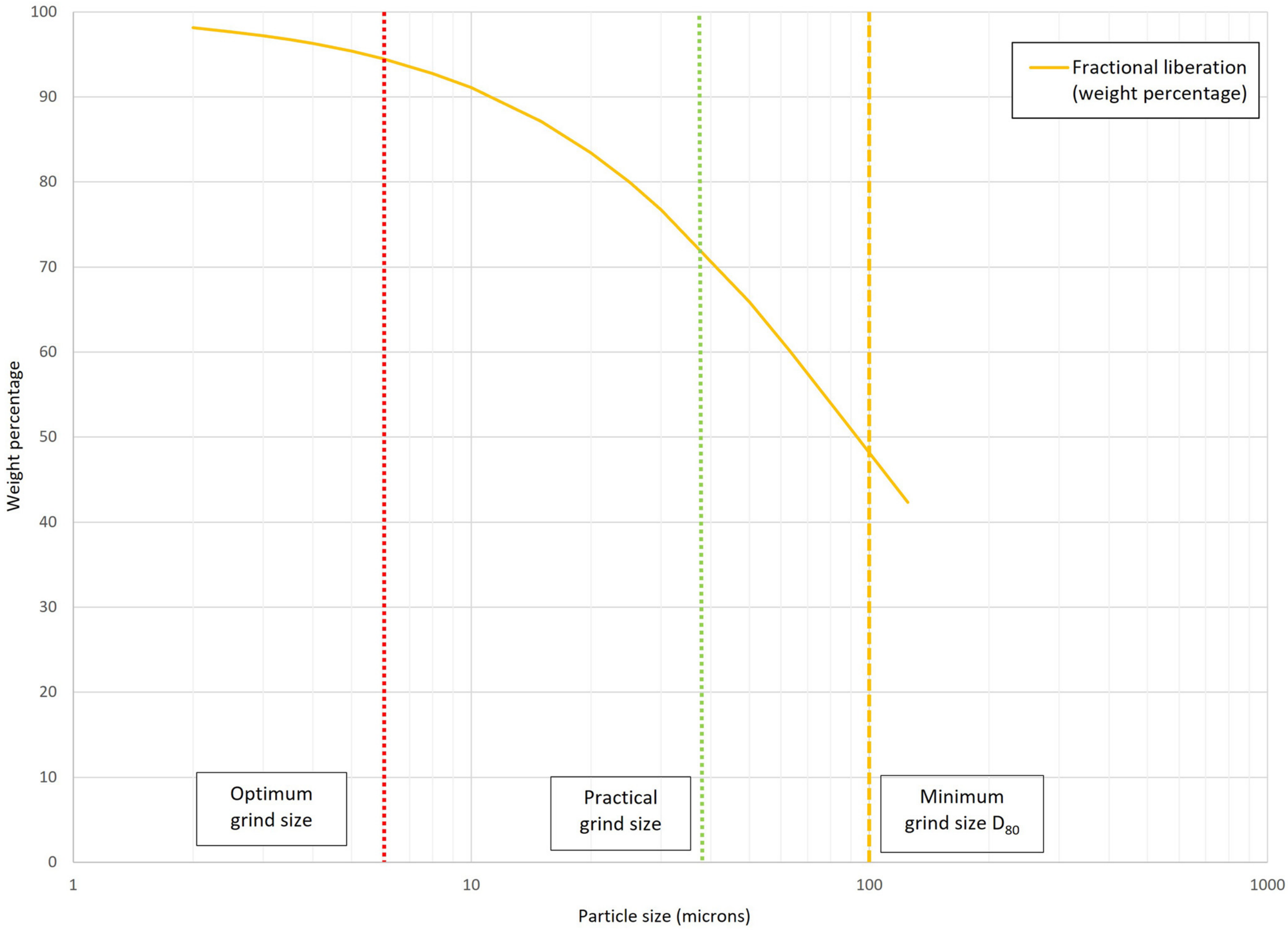

Fig. 7. Fractional liberation and grind sizes for gold in ore, Migori County, Kenya.

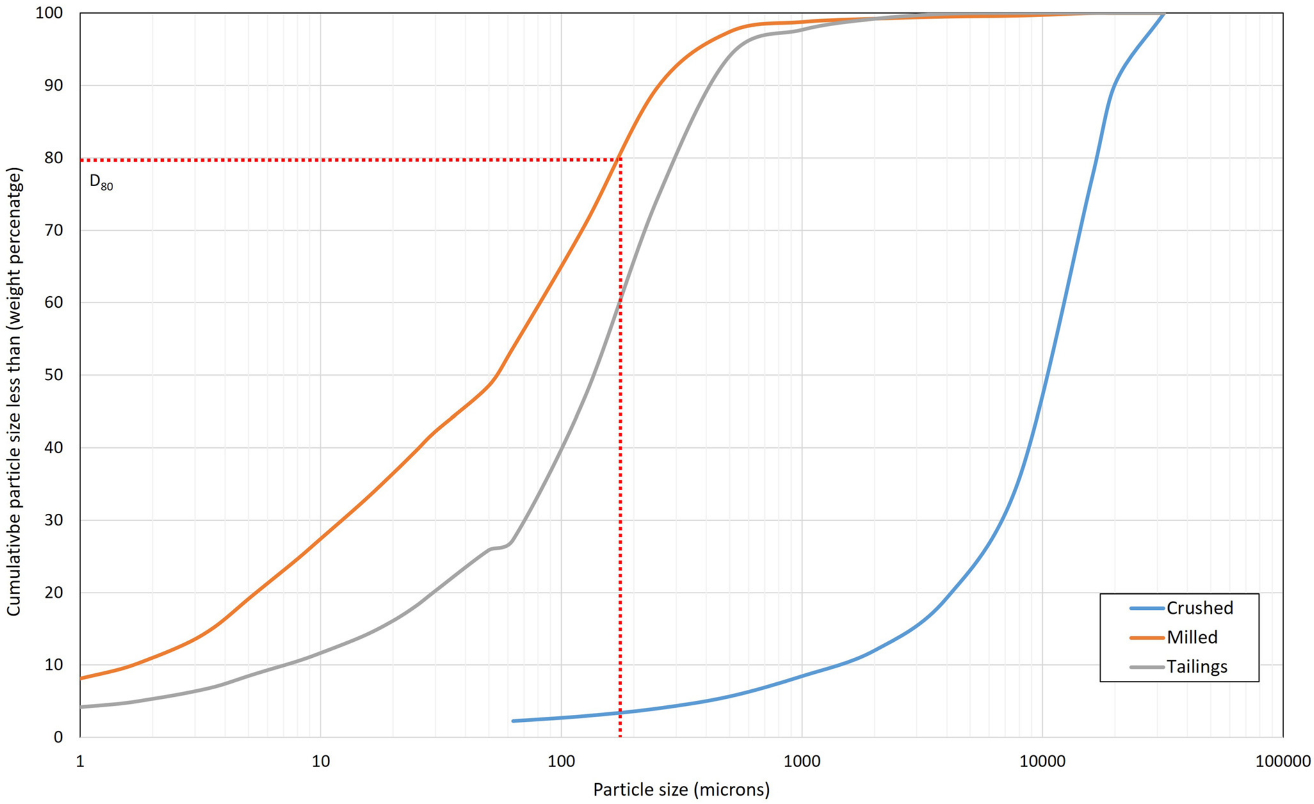

Fig. 8. Particle size distribution of artisanal and small-scale gold mining processing products, Migori County, Kenya.

Table 5. Gold content of ore and mining products, Migori County, Kenya

Gold content	Crushed ore (g t^{-1})	Milled ore (g t^{-1})	Tailings (g t^{-1})	Concentrate (g t^{-1})	Concentration ratio
ASGM sites	7.1 (0.9–23.9)	17.6 (4.4–50.7)	5.0 (1.8–11.1)	49.1 (39.1–64.4)	2.5 (0.9–7.6)
MICA plant	10.2 (1.5–18.9)	9.1 (5.2–12.9)	4.5 (1.9–7.0)	316.1 (66.6–565.9)	66.7 (28.8–170.9)

Mean data with data range given in brackets next to the mean values. Gold content is expressed as g t^{-1}, grams per tonne. The concentration ratio is the ratio of milled ore (feed) to concentrate gold contents. Data are based on eight crushed ore samples, eight milled ore samples, six ASGM sluice box and two MICA plant concentrate samples, and six ASGM sluice box and four MICA plant tailings samples. ASGM, Artisanal and small-scale gold mining; MICA, Migori County Artisanal Miners Co-operative.

is finer than 15 µm. This material is beyond the capability of gravity-based mineral processing methods such as sluice boxes and shaking tables. Reducing the residence time of the feed material in the mill and introducing a screen to remove ground material would help to reduce over-grinding.

- Gravity-based mineral processing is more effective with closely sized feed material using sluice boxes that are operated using conditions appropriate to the particle size of the feed. Steeper sluice deck angles and higher feed rates are more effective for coarse-grained feed. Shallower sluice deck angles and slower feed rates are more effective for fine-grained feed. Screening the milled ore into fine and coarse-grained material and processing them on separate sluice boxes tailored to the particle size of the feed material would improve gold recovery.
- Other good practices that may improve gold recovery include: increasing the length of the sluice box channel, using more efficient trapping medium on the sluice deck (such as expanded metal and nomad matting), thorough mixing of the feed slurry with water and a consistent, steady flow of feed slurry with no interruptions across the sluice deck. All of these modifications will help to create the separation conditions that ensure the capture of gold particles on the sluice deck rather than their loss into the tailings.
- In the medium to longer term, replacement of sluice boxes with shaking tables would have the most impact on the amount of gold recovered by artisanal-scale miners.

The Migori County Artisanal Miners Co-operative has established a small-scale gold processing facility to demonstrate good practice for gold recovery. The Migori County Artisanal Miners Co-operative gold processing plant includes a jaw crusher, hammer mill and shaking table. This shaking table has the capacity to recover gold down to a much smaller particle size than the sluice boxes used by the artisanal miners. The Migori County Artisanal Miners Co-operative also has a centrifugal (bowl) separator and a ball mill they plan to deploy in a second demonstration gold-processing circuit. Currently, gold production is around 100 g per day; the target is 500 grams per day. Tailings are sent to the MICA cyanide leaching plant; the gold content of the tailings is between 0.3 and 0.8 grams per tonne. Gold production from the cyanide leaching plant is approximately 1.2–1.5 kg per month.

The use of mercury to recover gold from concentrates in Migori is an issue that will be more intractable to solve. There are many long-standing technical solutions to help minimize the consumption of mercury, such as retorts to recover the mercury and mercury-free methods of recovering gold (UNEP 2012). A mercury retort has been produced by MICA for use by the artisanal miners to safely recover mercury from the amalgam. The MICA-produced retort is based on a retort from Zimbabwe and is manufactured locally in Migori town. Use of this retort would lead to a significant reduction in the amount of mercury being released into the environment and would also save money by reducing the amount of mercury required. The use of borax has been demonstrated to be very effective and environmentally benign (Appel and Na-Oy 2012). Elimination of mercury would remove the risks posed by the cyanidation of tailings, which leads to the formation of mercury cyanide complexes which are highly mobile and pose a significant risk to the environment (Seney *et al.* 2020).

The uptake of mercury-reduction solutions will rely on the success of small-scale mining cooperatives such as MICA in promoting good practice for gold recovery and building on the success of past technology transfer. The Tanzanian ball mill, which was introduced by MICA and is now ubiquitous across Migori, is an example of highly successful good practice implementation. Future good practice implementation by MICA will focus on the use of shaking tables for fine gold recovery and retorts for mercury recovery.

Adopting improved ASGM practices would increase the recovery of fine-grained gold, reduce the amount of mercury consumed and potentially reduce the amount of cyanide used in the recovery of gold lost into tailings. Improved ASGM practices have the potential to provide a significant boost to local economies securing livelihoods and enhance the quality of life for many communities. Reducing the amount of mercury used would contribute to the aspirations of the UN Minamata Convention on Mercury, of which Kenya is a signatory, to eliminate the use of mercury, formalize the ASGM sector, introduce good practice and protect the health of mining communities (UNEP 2012). Adopting improved mining practices would address the UN Sustainable Development Goals (SDGs), in particular, SDG 1 to end poverty, SDG 6 to ensure the availability and sustainable management of water, SDG 8 to promote sustainable economic growth and SDG 15 to protect, restore and promote sustainable use of terrestrial ecosystems respectively (United Nations 2018; World Bank 2019).

Conclusions

This study set out to achieve a better understanding of the particle size properties of the gold worked in the artisanal gold mining district of Migori in Kenya. The gold present in the Archean greenstone ore is shown by SEM grain count analysis to be very fine grained, with an average particle size of 3.5 µm. This is far too fine grained for effective recovery by the sluice boxes used by the artisanal gold miners in Migori, as sluice boxes are largely ineffective for gold finer than 100 µm. However, taking the weight of the gold into consideration, the mid-point in the weight distribution of the gold is 45 µm. This is significant as, even though this is still too fine for sluice boxes, it does indicate that a significant proportion of the gold could be recovered using an alternative gravity-based mineral processing method such as a shaking table (effective recovery range from 15 to 3000 µm).

Implementation of good mining practice would undoubtedly improve the amount of gold recovered and reduce the amount of mercury consumed by the existing artisanal gold mining operations. However, a more fundamental shift away from sluice boxes to shaking tables would be needed to achieve a more significant increase in the amount of gold recovered. The good mining practices demonstrated by the mining cooperative MICA, such as shaking tables and retorts to recover mercury, are likely to be the most effective means of successfully improving gold recovery and reducing mercury consumption in the artisanal gold mining district of Migori.

Scientific editing by Gene Rankey

Acknowledgements This paper is part of research by the British Geological Survey in collaboration with the University of Nairobi and the Migori County Artisanal Miners Co-operative to promote good practice, reduce mercury use and improve gold recovery using appropriate technology in Artisanal and Small-scale Gold Mining districts. It was part of the project 'From source to sink: Quantifying the local and downstream environmental impacts of ASGM'. The Migori County Artisanal Miners Co-operative facilitated visits and assisted with negotiations for collection of samples in the artisanal mining areas in Migori County, Kenya.

The authors would like to thank the following for their active support and encouragement: Professor Eric Odada, Professor Daniel Ichang'i, Dr Lydia Olaka and Jemimah Muluu, Department of Geology, University of Nairobi; John Asembo and James Asembo, Migori County Artisanal Miners Co-operative; Terry Garde and Joshua Read, Mining Engineers; Ellie Evans, Dr Joseph Mankelow, Dr Michael Watts, Dr Andy Marriott, Dr Barbara Palumbo-Roe, Eimear Deady and Richard Shaw, British Geological Survey.

This paper is published with the permission of the Director of the British Geological Survey.

Author contributions **CJM**: conceptualization (lead), data curation (lead), formal analysis (lead), investigation (lead), methodology (equal), project administration (lead), supervision (lead), writing – original draft (lead), writing – review & editing (equal); **TB**: investigation (supporting), writing – original draft (supporting), writing – review & editing (equal); **CO**: investigation (supporting); **MN**: writing – review & editing (supporting); **JCR**: investigation (supporting), writing – review & editing (supporting); **CK**: methodology (supporting), writing – review & editing (supporting); **MP**: investigation (supporting), writing – review & editing (supporting).

Funding This research was supported by BGS NC-ODA grant NE/R000069/1 entitled Geoscience for Sustainable Futures. It was delivered via the BGS Eastern Africa Official Development Assistance Research Platform.

Competing interests The authors declare that they have no known competing financial interests or personal relationships that could have appeared to influence the work reported in this paper.

Data availability The datasets generated during and/or analysed during the current study are not publicly available as they have not been published elsewhere but are available from the corresponding author on reasonable request.

References

Anhaeusser, C.R. 2014. Archaean greenstone belts and associated granitic rocks – a review. *Journal of African Earth Sciences*, **100**, 684–732, https://doi.org/10.1016/j.jafrearsci.2014.07.019; http://www.sciencedirect.com/science/article/pii/S1464343X14002374

Appel, P.W. and Na-Oy, L. 2012. The borax method of gold extraction for small-scale miners. *Journal of Health and Pollution*, **2**, 5–10, https://doi.org/10.5696/2156-9614-2.3.5

Borg, G. and Shackleton, R. 1997. The Tanzania and NE-Zaire cratons. *Oxford Monographs on Geology and Geophysics*, **35**, 608–619.

Buchholz, P., Herzig, P., Friedrich, G. and Frei, R. 1998. Granite-hosted gold mineralization in the Midlands greenstone belt: a new type of low-grade gold deposit in Zimbabwe. *Mineralium Deposita*, **33**, 437–460, https://doi.org/10.1007/s001260050162

DuBois, C.G.B. and Walsh, J. 1970. *Minerals of Kenya*. Geological Survey of Kenya.

Finch, J.A. and Petruk, W. 1984. Testing a solution to the King liberation model. *International Journal of Mineral Processing*, **12**, 305–311, https://doi.org/10.1016/0301-7516(84)90036-X; https://www.sciencedirect.com/science/article/pii/030175168490036X

Foster, R. and Piper, D. 1993. Archaean lode gold deposits in Africa: crustal setting, metallogenesis and cratonization. *Ore Geology Reviews*, **8**, 303–347, https://doi.org/10.1016/0169-1368(93)90021-P

Gan, S. and Van Reenen, D. 1997. Geology of gold deposits in the Southern Marginal Zone of the Limpopo belt and adjacent Sutherland greenstone belt, South Africa: Klein Letaba. *South African Journal of Geology*, **100**, 73–83.

Huddelston, A. 1951. *Geological Map of the Kisii District. Map at 1:125 000*. Mining and Geology Department, Kenya.

Ichang'i, D.W. 1993. Lithostratigraphic setting of mineralisation in the Migori Segment of the Nyanza Greenstone belt. Proceedings of the Fifth Conference on the Geology of Kenya on Geology for Sustainable Development. Geological Society of Kenya, 78–84.

Ichang'i, D. and MacLean, W. 1991. The Archean volcanic facies in the Migori segment, Nyanza greenstone belt, Kenya: stratigraphy, geochemistry and mineralization. *Journal of African Earth Sciences*, **13**, 277–290, https://doi.org/10.1016/0899-5362(91)90091-C

Intergovernmental Forum on Mining Minerals Metals and Sustainable Development 2017. *Global Trends in Artisanal and Small-Scale Mining (ASM): A Review of Key Numbers and Issues*. Winnipeg.

Kalleske, N.L. 2010. *Mineralogical and Petrogenetic Study of Gold Ore from the Boddington Gold Deposit*. WA thesis, BSc (Hons), University of Adelaide, School of Earth and Environmental Sciences.

Kinabo, C. 1991. Critical evaluation of small-scale gold plants in Africa, with special reference to Geita gold plant, Tanzania. *In: African Mining 91*. Springer, 147–157, https://doi.org/10.1007/978-94-011-3656-3_15

King, R. 1979. A model for the quantitative estimation of mineral liberation by grinding. *International Journal of Mineral Processing*, **6**, 207–220, https://doi.org/10.1016/0301-7516(79)90037-1

Kinnunen, A. 2008. *Palaeoproterozoic high-sulphidation epithermal gold deposit at Orivesi, southern Finland*. Masters thesis, Faculty of Science, Department of Geoscience, University of Oulu.

Lukonin, D. 2008. *Archean and Proterozoic gold deposits of the Fennoscandian Shield*. Master's thesis, Lulea Universtiy.

Mitchell, C., Evans, E. and Styles, M. 1997. *A review of gold particle-size and recovery methods*. Technical Report **WG/97/14**. British Geological Survey, Nottingham.

Mitchell, C.J., Bide, T. and Odhiambo, C. 2023. Recovering the lost gold of the developing world: case study in Migori County, Kenya. *In:* Wardrop, D. (ed.) Proceedings of the 22nd Extractive Industry Geology Conference 2022 and Technical Meeting 2023. Extractive Industry Geology, 98–104, https://nora.nerc.ac.uk/id/eprint/538617/

Mériaud, N. and Jébrak, M. 2017. From intrusion-related to orogenic mineralization: the Wasamac Deposit, Abitibi Greenstone Belt, Canada. *Ore Geology Reviews*, **84**, https://doi.org/10.1016/j.oregeorev.2017.01.021

Ogola, J.S. 1987. Mineralization in the Migori greenstone belt, Macalder, western Kenya. *Geological Journal*, **22**, 25–44, https://doi.org/10.1002/gj.3350220605

Ogola, J.S. 1993. Fluid inclusion studies on auriferous quartz from the greenstone complexes of western Kenya. Proceedings of the Fifth Conference on the Geology of Kenya on Geology for Sustainable Development. Geological Society of Kenya, 47–56.

Ogola, J.S., Mitullah, W.V. and Omulo, M.A. 2002. Impact of gold mining on the environment and human health: a case study in the Migori gold belt, Kenya. *Environmental Geochemistry and Health*, **24**, 141–157, https://doi.org/10.1023/A:1014207832471

Petruk, W. 1986. Predicting and measuring mineral liberations in ores and mill products, and effect of mineral textures and grinding methods on mineral liberations. *In:* R.D. Hagni (ed) *Process Mineralogy VI*. AIME/TMS, Warrendale, PA, 393–403.

Sanders, L.D. 1964. *Copper in Kenya*. Government of Kenya.

Seney, C.S., Bridges, C.C. *et al.* 2020. Reaction of cyanide with Hg0-contaminated gold mining tailings produces soluble mercuric cyanide complexes. *Chemical Research in Toxicology*, **33**, 2834–2844, https://doi.org/10.1021/acs.chemrestox.0c00211

Shackleton, R.M. 1945. *Geology of the Migori Gold Belt and Adjoining Areas*. Geological Survey of Kenya.

Styles, M., Simpson, J. and Steadman, E. 2002. *Good practice in the design and use of large sluice boxes*. Internal Report **CR/02/029N**. British Geological Survey.

UNEP 2012. *Reducing Mercury Use in Artisanal and Small-scale Gold Mining: A Practical Guide*. United Nations Environment Programme & Artisanal Gold, https://web.unep.org/globalmercurypartnership/reducing-mercury-use-artisanal-and-small-scale-gold-mining-practical-guide%C2%A0

UNEP 2019. *Minamata convention on mercury: text and annexes*. United Nations Environment Programme, Nairobi, Kenya. https://minamataconvention.org/sites/default/files/documents/information_document/Minamata-Convention-booklet-Sep2019-EN.pdf

United Nations 2018. *Global Indicator Framework for the Sustainable Development Goals and Targets of the 2030 Agenda for Sustainable Development*. World Bank, Geneva, https://unstats.un.org/sdgs/indicators/indicators-list/

Wang, C., Shao, Y., Huang, K., Zhou, H., Zhang, J., Liu, Z. and Liu, Q. 2018. Ore-forming processes at the Xiajinbao gold deposit in Eastern Hebei Province: constraints from EPMA and LA-ICPMS analysis. *Minerals*, **8**, 388, https://doi.org/10.3390/min8090388

World Bank 2019. *State of the Artisanal and Small-Scale Mining Sector*. World Bank, Washington, DC.

Yuan, Y.-s., Li, S.-p. *et al.* 2019. An integrated ore prospecting model for the Nyasirori gold deposit in Tanzania. *China Geology*, **2**, 407–421, https://doi.org/10.31035/cg2018127